Microscopic Mechanism of 1/*f* Noise in Graphene: Role of Energy Band Dispersion

Atindra Nath Pal,[†,]* Subhamoy Ghatak,[†] Vidya Kochat,[†] E. S. Sneha,[†] Arjun Sampathkumar,[‡] Srinivasan Raghavan,[‡] and Arindam Ghosh[†]

[†]Department of Physics and [‡]Materials Research Center, Indian Institute of Science, Bangalore 560 012, India

ABSTRACT A distinctive feature of single-layer graphene is the linearly dispersive energy bands, which in the case of multilayer graphene become parabolic. A simple electrical transport-based probe to differentiate between these two band structures will be immensely valuable, particularly when quantum Hall measurements are difficult, such as in chemically synthesized graphene nanoribbons. Here we show that the flicker noise, or the 1/*f* noise, in electrical resistance is a sensitive and robust probe to the band structure of graphene. At low temperatures, the dependence of noise magnitude on the carrier density was found to be opposite for the linear and parabolic bands. We explain our data with a comprehensive theoretical model that clarifies several puzzling issues concerning the microscopic origin of flicker noise in graphene field-effect transistors (GraFET).

KEYWORDS: graphene · noise · multilayer · 1/*f* noise · charge impurity scattering

Both single-layer and multilayer graphene have drawn immense attention in the field of nanoelectronics. The electronic properties of graphene flakes are modified drastically with the number of layers.[1−4] The single-layer graphene (SLG) is a zero gap semiconductor with linear band structure, while bilayer graphene is the same with parabolic bands.[3] Trilayer graphene, on the other hand, shows semimetallic behavior.[4] Except for the quantum Hall effect,[1,2] the distinction between linear and parabolic bands has been very hard to capture in electrical transport. With new techniques of realization of graphene directly in nanostructured form,[5,6] this issue is becoming progressively important. Knowing the band dispersion relation can separate single-layer graphene from the multilayered ones. The existing techniques, such as the Raman spectroscopy[7] and atomic force microscopy, are not very convenient for application in nanoscale devices. Techniques based on Auger electron spectroscopy[8] or scanning electron microscopy[9] are not absolute measures of thickness of graphene and depend on prior calibration.

The flicker noise in electrical transport is generally a nuisance in the operation of a field-effect device. This noise manifests in slow fluctuations in the drain−source current due to the fluctuations in the channel conductivity, σ. The flicker noise is often called the 1/*f* noise because of its power spectral density, $S_\sigma(f) \propto 1/f^\nu$, where *f* is frequency and $\nu \approx 1$. The 1/*f* noise has been studied extensively in metal oxide field-effect transistors (MOSFET), where the trapping and detrapping of charge at the channel−oxide interface leads to 1/*f*-type fluctuations in σ.[10] Similar mechanisms of noise have been assumed for carbon nanotube field-effect devices, as well,[11] where the trapping events close to the nanotube−metallic lead Schottky barriers cause fluctuations in the effective gate voltage.[12] In all cases, the magnitude of noise reflects the ability of the conducting channel to screen the external potential fluctuations at the traps. This in turn depends on the density of states and energy dispersion characteristics of the channel. In this paper, we have explored if this property of 1/*f* noise can probe the band structure of graphene.

In spite of several recent reports of noise measurement, the microscopic understanding of noise in GraFETs is rather limited.[13−21] The carrier density (*n*) dependence of noise magnitude was found to be opposite for single- and bilayer graphene nanoribbons[13] but not necessarily in extended graphene flakes.[18,19] Formation of a gate electric field-induced energy gap has been suggested to explain the increase in noise magnitude with increasing *n* in bilayer graphene,[13,14] but this picture cannot explain the behavior of noise in thicker devices.[15] A quantitative model to understand the noise in variety of GraFET also does not exist. The augmented charge noise model for carbon nanotubes,[22] which does not consider the graphene band structure explicitly, also fails to describe the carrier density (*n*) dependence of noise in

*Address correspondence to atin@physics.iisc.ernet.in.

Received for review November 29, 2010 and accepted January 26, 2011.

Published online February 18, 2011
10.1021/nn103273n

TABLE 1. Details of the Devices

device	growth	layer	substrate	device area (L × W) (μm^2)	mobility (cm^2/V·s)
Ex-Ox-SLG1	exfoliation	1	SiO_2	4.5 × 3.5	8000
Ex-Ox-SLG4	exfoliation	1	SiO_2	3.1 × 5	3500
Ex-Ox-BLG2	exfoliation	2	SiO_2	1.2 × 5.2	1200
Cvd-Ox-SLG2	CVD	1	SiO_2	15 × 60	400
Ex-Sus-SLG	exfoliation	1	suspended	1.5 × 2	20000
Ex-Ox-FLG	exfoliation	3−4	SiO_2	2 × 3	2450
Ex-Ox-MLG	exfoliation	14−15	SiO_2	1.9 × 6	1200

most single-layer graphene (SLG) devices close to charge neutrality point (the Dirac point).[13,15] The influence of quenched disorder, and related charge inhomogeneity,[23] which are both very serious technological bottlenecks, is also not known.

Hence a comprehensive experimental approach, aided with a microscopically intuitive modeling, is required to understand the influence of graphene band structure on the low-frequency noise. To achieve this, we have fabricated seven different types of graphene field-effect devices, which include exfoliated single- and multilayer graphene on an oxide substrate, freely suspended single-layer graphene, and chemical vapor deposition (CVD)-grown graphene on SiO_2 (see Table 1 for details). The substrated graphene flakes were prepared on the usual 300 nm SiO_2 on n^{++}-doped silicon substrate (the backgate) by micromechanical exfoliation of natural graphite (NGS Naturgraphit GmbH). In all cases, we have used RCA cleaning of the substrate and standard electron beam lithography technique followed by thermal evaporation of 40−50 nm gold (99.99%) to fabricate the devices. For a suspended graphene transistor, 100 nm thick gold electrodes were made, followed by etching of the underneath oxide by 1:6 buffered HF solution for 2.5 min. Finally, the devices were released in a critical point dryer. No current annealing or Ar/H_2 annealing was used in our experiments to remove the acrylic residues in any of the devices. To avoid large electrostatic force in the suspended device, only a small range of gate voltage was scanned, corresponding to $n \lesssim 2 \times 10^{11}$ cm^{-2}. The CVD graphene was grown by thermal decomposition of methane on 25 μm thick copper foil at 1000 °C.[24] Methane was introduced into the chamber at a rate of 35 sccm and a pressure of 4 Torr for a growth time of 8 min, after which the chamber was cooled to room temperature. The susbsequent processes involved PMMA coating, dissolving copper foil with ferric chloride (1.75 g of $FeCl_3$/5 mL of conc. HCl/50 mL deionized water), transfer onto the Si/SiO_2 substrate, coating a second PMMA layer, and finally cleaning with acetone/IPA. Noise in the graphene devices was measured in low-frequency ac four- and two-probe methods in a high vacuum environment. See ref 25 for details. The excitation was kept below 50 μA to avoid heating and other nonlinearities and verified by quadratic excitation dependence of voltage/current noise at a fixed resistance R. The background noise was measured simultaneously and subtracted from the total noise.

RESULTS AND DISCUSSION

The main components of the experiment are shown in Figure 1, illustrated with a typical exfoliated SLG device (Ex-Ox-SLG1) on the Si/SiO_2 substrate (see Table 1 for device details). A cartoon of the device structure is shown in Figure 1a (top schematic), and its actual structure resembles the micrograph in Figure 2a1. The n dependence of σ was measured first, which shows σ to vary linearly at low $|n|$, indicating charged impurity scattering (inset of Figure 1c). For noise measurements, the gate voltage (*i.e.*, n) was held constant and σ was measured as a function of time. The normalized fluctuations, $\delta\sigma/\sigma$, peak at the Dirac point, as evident in the time traces in Figure 1b. We find $S_\sigma(f) \propto 1/f$ at all n, confirming the $1/f$ nature of noise (Figure 1c). Both four- and two-probe measurements yielded the same results, indicating negligible contribution from contact noise. S_σ/σ^2 decreases monotonically as $|n|$ is increased on both electron- and hole-doped sides (Figure 1d). The noise magnitude decreases by more than 1 order of magnitude at high n and agrees with recent reports on similar devices.[13,15,18,19]

The specific nature of n dependence of noise was, however, found to be dependent on disorder. To illustrate this, we have compared three different classes of SLG with varying levels of quenched disorder. The experiments, with over 50 devices, were carried out on (1) mechanical exfoliation on SiO_2 substrate (Ex-Ox-SLG4, Figure 2a1−a3, similar to but with mobility lower than Ex-Ox-SLG1), (2) chemical vapor deposition (Cvd-Ox-SLG2, Figure 2b1−b3), and (3) suspending mechanically exfoliated SLG (Ex-Sus-SLG, Figure 2c1−c3) across a trench. The Raman spectra (Figure 2a2,b2,c2) are shown not only to identify the monolayers but also to compare the disorder levels. For Cvd-Ox-SLG2, the transfer process onto the SiO_2/Si substrate introduces considerable disorder, both structural (ruptures/voids) and foreign charged/uncharged residues (see the electron micrograph and the disorder (D) peak in the Raman spectrum in Figure 2b2), resulting in rather poor $\mu \sim 400$ cm^2/V·s (see Table 1). Interestingly, noise does not seem to be affected much by these static disorder, showing comparable noise magnitude in both exfoliated and CVD-grown graphene (see Figure 2). Two important points need to be noted in Figure 2: (1) At large $|n|$, noise decreases with increasing $|n|$ in all SLG devices at all T down to 80 K. (2) At low $|n|$, the behavior of noise in substrated SLG devices (including Ex-Ox-SLG1 in Figure 1d) is similar, and S_σ/σ^2 shows a peak at

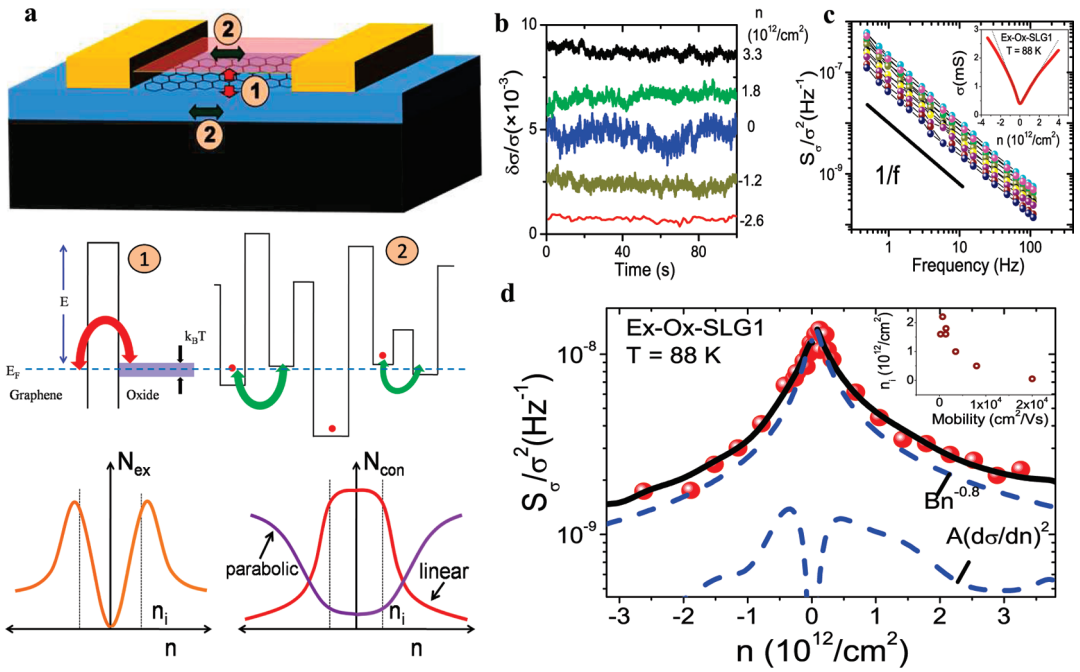

Figure 1. (a) Schematic of the GraFET device showing two different charge noise mechanisms. Process (1) corresponds to the exchange noise due to the charge transfer between graphene and its environment. Process (2) depicts the configuration noise arising from the rearrangement of trapped charges within the environment. The density dependence of each component has been schematically shown at the bottom depicting opposite nature of configuration noise for linear and parabolic bands. (b) Time domain conductivity fluctuations at different carrier densities. (c) Typical noise power spectra S_σ/σ^2 at various back gate voltages, showing 1/*f* characteristics. Inset shows conductivity (σ) *vs* density (*n*) for a substrated SLG device, with the dotted line indicating the linear region. (d) S_σ/σ^2 (at 1 Hz) *vs* density (*n*) data for a substrated SLG device, fitted with eq 1 (see text). The contributions from the two different noise mechanisms are shown by the dashed lines. Inset shows the plot of n_i *vs* mobility from various single-layer devices.

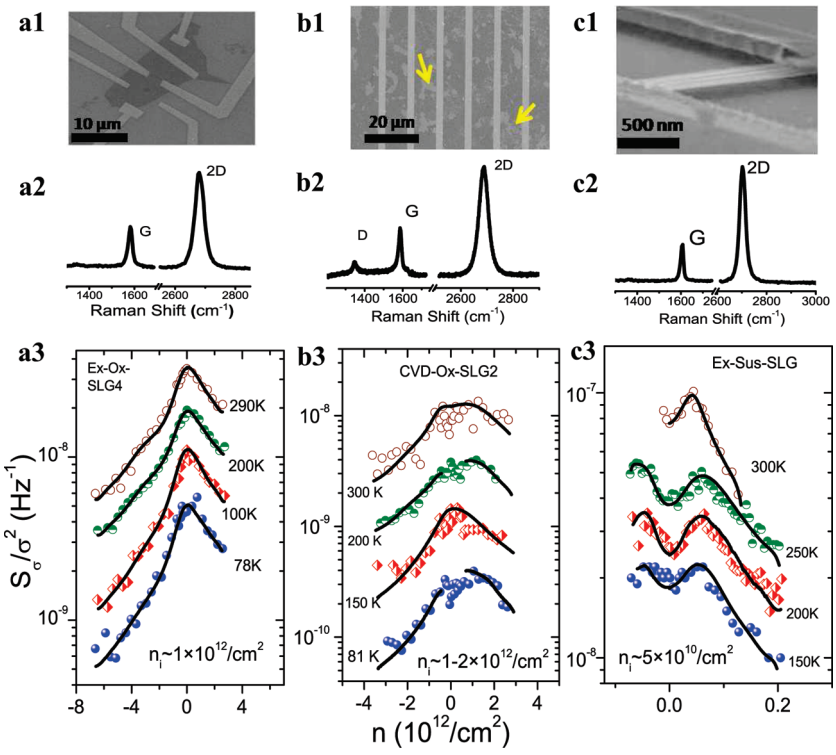

Figure 2. Noise magnitude, S_σ/σ^2 (at 1 Hz) *vs* carrier density (*n*) at different temperatures, fitted with the FCD model for substrated SLG, CVD graphene, and suspended SLG in panels a3−c3, respectively. The top panel (a1−c1) shows the SEM images of the devices and corresponding Raman spectrum for each device is shown in a2−c2. For clarity, the noise traces at different temperatures have been shifted vertically. The arrows in b2 indicate typical voids and ruptures in CVD graphene.

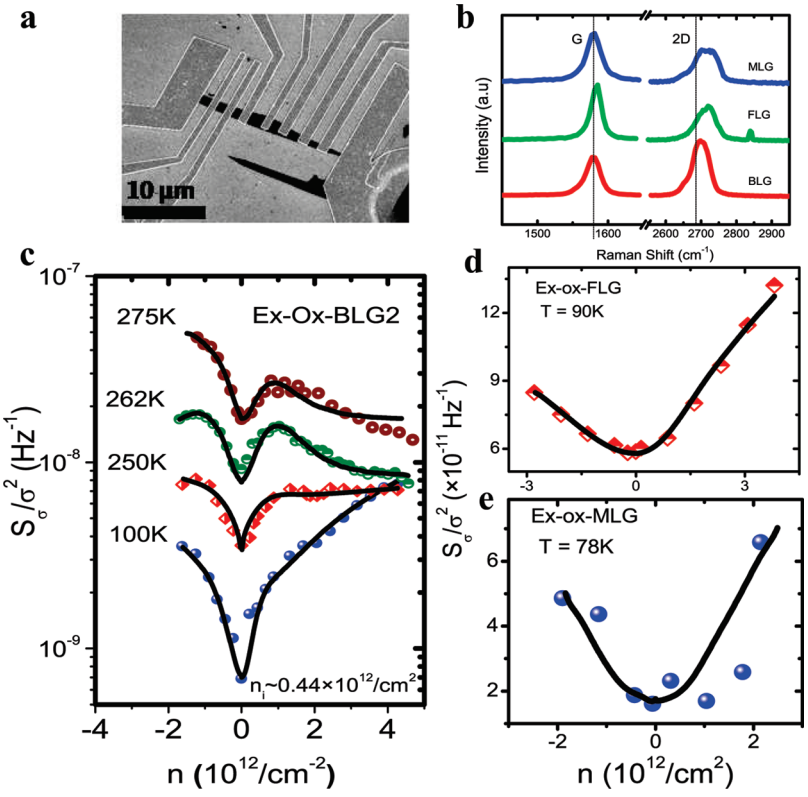

Figure 3. (a) SEM micrograph of the BLG device used in the experiment. (b) Raman spectra for BLG, FLG, and MLG showing the characteristic G and 2D peaks. (c) Noise magnitude, S_σ/σ^2 (at 1 Hz), *vs* carrier density (n) at different temperatures, fitted with the FCD model for the BLG device, while similar plots have been shown for FLG ($T = 90$ K) and MLG ($T = 78$ K) devices in panels d and e, respectively.

the Dirac point, but in the suspended graphene, where disorder was significantly reduced, a nonmonotonic dependence of noise on n is observed (Figure 2c3).

Before analyzing the behavior of noise in SLG quantitatively, we focus on the bilayer (BLG), few-layer (FLG), and many-layer (MLG) graphene devices, where noise measurements led to strikingly different results. Figure 3a shows a micrograph of the BLG device, and Figure 3b presents the corresponding Raman spectrum along with those of FLG (∼3−4) and MLG (∼15). The BLG (Ex-Ox-BLG2), FLG (Ex-Ox-FLG), and MLG (Ex-Ox-MLG) devices were obtained by exfoliation of graphite on identically treated SiO_2/Si substrates. In the BLG device, the intrinsic electron doping restricted us only to the electron-doped region for detailed $1/f$ noise measurements. S_σ/σ^2 in the BLG device clearly behaves very differently from the SLG devices in Figure 2, particularly at low T. At $T \lesssim 150$ K, S_σ/σ^2 increases monotonically with $|n|$, in agreement with our earlier results,[14] but becomes nonmonotonic at higher T, similar to the results reported by Heller *et al.*[18] The low-T behavior of noise in FLG and MLG is same as that in BLG, indicating this to be a feature of graphene devices with parabolic bands. In the past, the increase in noise with $|n|$ in BLG was attributed to reduction in screening due to opening of a band gap,[13,14] but similar behavior in FLG and MLG indicates such a description to be inadequate. At higher T, the noise in BLG becomes nonmonotonic in $|n|$, with partial resemblance to the suspended SLG devices. Nevertheless, the n dependence of noise at moderately low T (∼100 K) can clearly distinguish between the single- and multilayered graphene.

We will now construct a general theoretical framework which establishes that the n dependence of noise is an intrinsic property, connected to graphene's band structure. We consider the generic GraFET structure in the schematic of Figure 1a, where the local environment of the graphene film consists of the underlying insulating substrate and surface adsorbates (or top gate dielectric, if any). Focusing on the noise that arises due to fluctuating charge distribution (FCD) around the graphene film, two processes are identified: (1) Exchange of charge between graphene and its environment, for example, through trapping−detrapping process, which involves time-dependent changes in n. This causes a charge exchange noise, $N_{ex} \propto (d\sigma/dn)^2$, through correlated number and mobility (μ) fluctuations.[10] (2) The second process consists of a slow rearrangement of charge within the local environment of graphene, for example, random migration of trapped charges within the substrate or surface adsorbates (process 2 in the schematic in Figure 1a), and is referred to as configuration noise (N_{con}). This process alters the disorder landscape due to Coulomb potential from

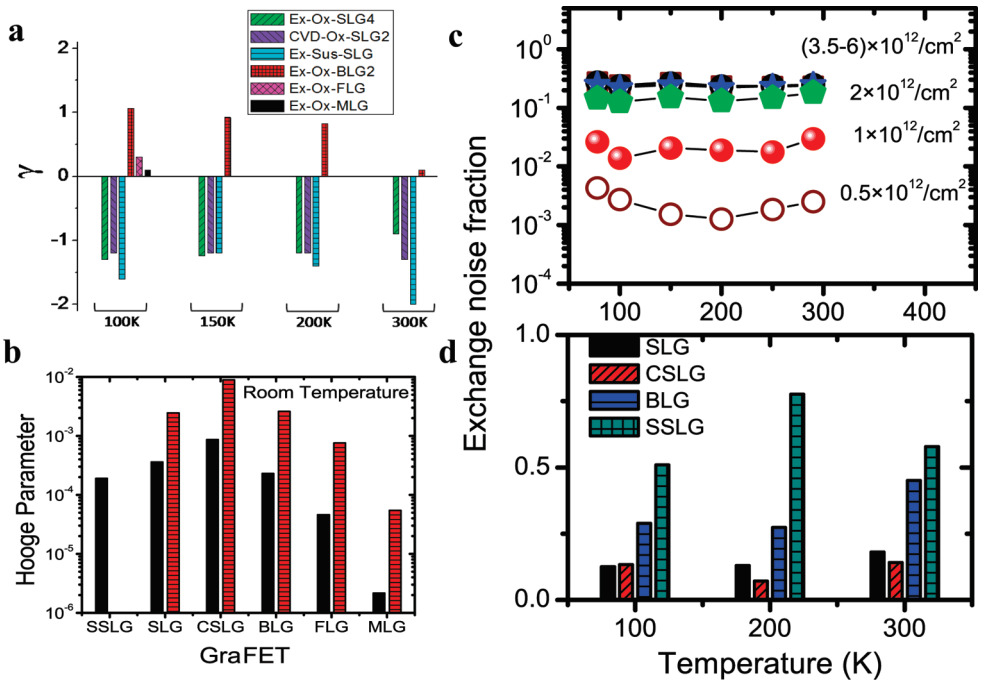

Figure 4. (a) Value of γ (see text) at different temperatures, for devices used in this work. (b) Comparison of Hooge parameter (γ_H) for various GraFET devices at room temperature: suspended single-layer graphene (SSLG), substrated single-layer (SLG), bilayer (BLG), few-layer (FLG), many-layer (MLG), and CVD-grown single-layer graphene (CSLG). The solid black bar and dashed red bar correspond to γ_H measured at densities of $n = 2 \times 10^{11}$ and 2.4×10^{12} /cm^2, respectively. (c) Exchange noise fractions are plotted with temperature at different carrier densities (n) for the SLG device used in Figure 2a1−a3. (d) Exchange noise fractions for four different kinds of GraFETs at three different temperatures at a carrier density of $n = 2n_i$ (see text).

trapped charges leading to random fluctuations in the scattering cross section (Λ_c). Within a "local interference" framework,[26] $\delta\Lambda_c \sim \Lambda_c \propto |v_q|^2$, where v_q is the screened Coulomb potential of the trapped charge. Thus at large n, $N_{con} \propto l^2|v_q|^4 \sim |n|^\gamma$, where l is the mean scattering length.[26] γ is determined by the n dependence of l and v_q and hence is sensitive to the nature of graphene band structure. When Boltzmann transport in Thomas−Fermi screening is assumed, the total normalized noise power spectral density can be written as (see the Methods section for detailed derivation)

$$S_\sigma(f)/\sigma^2 = A(T)(d\sigma/dn)^2 + B(T)N_c(n) \qquad (1)$$

The parameters $A(T)$ and $B(T)$ are independent of n irrespective of the band structure but depend on T. The configuration noise is represented by the function $N_c(n) = |n|^\gamma$ for $|n| > n_i$, while for $|n| < n_i$, $N_c(n) =$ constant. Here n_i is the characteristic density scale at which charge distribution in graphene becomes inhomogeneous (see schematic in Figure 1a). In analyzing the noise data, the parameters A, B, n_i, and γ were kept as fitting parameters, and $d\sigma/dn$ was obtained from the $\sigma-n$ data. Due to particle−hole asymmetry,[27] the electron- and hole-doped regimes were fitted separately.[28]

Fitting eq 1 yields excellent agreement with the observed noise data in all devices, although the relative contributions of N_{ex} and N_{con} may vary significantly. For example, in device Ex-Ox-SLG1 (Figure 1d), N_{con} exceeds N_{ex} at all n, particularly at lower $|n|$ (dashed lines). Indeed, the peak in S_σ/σ^2 at the Dirac point can be attributed to larger configurational noise, that is, enhanced sensitivity of graphene to alteration in disorder landscape, with charge noise being minimal since σ varies weakly with n in this regime. Another key factor to note is that the fit yields $\gamma \sim -1.0$, which was found to be generic to other SLG devices, as well (see Figure 4a). As explained in the Methods section, this value of γ reflects screening (within Thomas−Fermi approximation) by the linear energy bands of SLG graphene. The magnitude of n_i ($\approx 1-3 \times 10^{12}$ cm^{-2}) in Cvd-Ox-SLG2 is significantly larger than typical n_i in exfoliated SLG devices and decreases with increasing mobility of the devices (see inset of Figure 1d). For Cvd-Ox-SLG2, significant electron−hole asymmetry due to impurity scattering leads to asymmetric noise behavior. It is remarkable that, in spite of higher level of structural disorder, noise in CVD-grown graphene continues to be dominated by fluctuating charge distribution, indicating that migration of structural disorder is mostly frozen well up to the room temperature. The qualitatively different n dependence of noise in the suspended device (Ex-Sus-SLG) can be readily understood from much smaller contribution of N_{con} with respect to N_{ex} due to the absence of a substrate (see Figure 4d). We believe the observed noise in our suspended graphene device to be due to residual surface contamination, in particular, the residues of the

electron beam resist (PMMA). The fact γ approaches ~ -2.0 near room temperature (Figure 4a) indicates a nearly constant l in these devices.

Equation 1 also describes the BLG (and FLG/MLG) noise data over the entire range of n rather well, albeit with a positive γ for all T. We find $\gamma \approx 1$ up to $T \sim 250$ K (Figure 4a). As shown in the derivation of eq 1 (Methods), the positive magnitude of γ reflects parabolic energy bands in BLG. The exact magnitude of γ for BLG, FLG, and MLG would depend on the n dependence of the scattering length l, which can be T-dependent, as well. For BLG, we find $\gamma \approx 1.0$ at low T but decreases to ~ 0.1 near room temperature, indicating a nearly constant l (Figure 4a). Thus the nonmonotonicity of BLG noise near room temperature essentially reflects the n dependence of $(d\sigma/dn)^2$ in these devices, as reported recently by Heller *et al.*[18]

In essence, graphene displays both trapping–detrapping-like noise in MOSFET (exchange noise) and that from changes in extended structural disorder as in disordered metal films (configuration noise). The origin of both in this case is a fluctuating charge distribution, where the sensitivity of configurational component (more specifically, γ) to band structure allows one to distinguish between the linear and parabolic bands (Figure 4a). In fact, we find the configurational component to dominate in most devices and densities, as indicated in Figure 4c, d but also depends on the quality of the substrate surface, roughness, nature of dielectric, operating n, *etc.* This can vary widely from one device to the other, helping us understand the apparently different experimental results on GraFET noise reported from different research groups.[13−21] Not surprisingly, the exchange noise is maximum in the suspended devices (Figure 4d), where the discontinuous layer of surface residues leaves very little room for the trapped charges to redistribute.

Figure 4b summarizes normalized noise levels in different designs of GraFET. The comparison is made in terms of the phenomenological Hooge parameter γ_H, defined as $\gamma_H = n(fS_\sigma)a_G/\sigma^2$, where a_G is the area of the graphene film between voltage leads. At all n, the substrated SLG devices, exfoliated or CVD-grown, are most noisy, whereas suspended SLG and thicker graphene systems are nearly a hundred times quieter. At room temperature, and even on a substrate, γ_H can be $\sim 10^{-7}-10^{-6}$ in FLG and MLG devices,[15] which are among the lowest known for metal or semiconductor nanostructures. The extreme low noise in these systems is due to strong screening by the lower layers, which also affects the gating ability, limiting their usefulness in active electronics, but makes them suitable as interconnects.

In conclusion, our experiments and microscopic model established low-frequency flicker noise as an excellent probe to graphene band structure. We focused on the carrier density dependence of noise and found that it behaves oppositely for the linear and parabolic band structure at moderately low temperatures. These results can be used to readily identify single-layer graphene from multilayered ones—a technique that can be particularly suitable for nanostructured graphene.

METHODS

Derivation of Equation 1. *Carrier Density (n) Dependence of Charge Exchange Noise.* We define charge exchange noise as the change $\delta\sigma$ in conductivity when a small number of charge δn is exchanged between graphene and its surroundings. As $\sigma = \sigma(n,\mu)$

$$\delta\sigma(t) = \frac{\partial\sigma}{\partial n}\delta n(t) + \frac{\partial\sigma}{\partial\mu}\delta\mu(t) \qquad (2)$$

According to the correlated carrier density−mobility fluctuation model of ref 10, $\delta\mu \sim \mu_{avg}^2 \sum \delta n$, where $\sum = \mu_C^{-1}/\delta n$ is related to the scattering rate entirely due to the Coulomb potential of the trapped charge δn located inside the substrate. Here, μ_C^{-1} and μ_{avg}^{-1} represent the Coulomb and net time-averaged scattering rates, respectively. Hence, the fluctuations in the conductivity $\delta\sigma(t)$ becomes

$$\delta\sigma(t) = \frac{\partial\sigma}{\partial n}\left(1 + \frac{\sigma}{e}\sum\frac{\partial \ln n}{\partial \ln \mu}\right)\delta n(t) \qquad (3)$$

The n dependence of $\sum$ can be calculated using semiclassical Boltzmann transport equation for 2D graphene, $\sigma = (2e^2/h)\text{-}k_F v_F \tau$, where k_F is the Fermi wave vector, v_F is the Fermi velocity of graphene carriers. Since $\sum$ is determined by the scattering time τ_C arising due to the Coulomb scattering only, we get

$$\sum = \frac{\pi}{e}\frac{n}{k_F v_F}\frac{\hbar/\tau_C}{\delta n_{tr}} \qquad (4)$$

where δn_{tr} is the trapped charge density at the graphene−substrate/dielectric interface due to charge exchange, that is, $\delta n_{tr} \sim \delta n$. Density dependence of $\sum$ can be obtained using the expressions for the scattering rates, calculated for both linear[29] and parabolic[30] band structures for Coulomb charge impurity scattering. For SLG, $1/\tau_C|_{SLG} \sim 1/\sqrt{n}$, while for BLG/MLG, $1/\tau_C|_{BLG} \sim n^0$. Incorporating these in eq 4, we find $\sum$ to be independent of density to the leading order for both linear and parabolic bands.

The power spectral density of conductivity noise can be calculated from eq 3 and will contain three terms.[10] The first term arises entirely due to number fluctuation; the second term describes the joint effect of both number and mobility fluctuation, and the final term represents the mobility fluctuation alone. Straightforward estimates show that the mobility fluctuation term dominates, and since $d \ln n/d \ln \mu$ is weakly varying and of order unity, the charge exchange noise term becomes

$$N_{ex} = A(T)\left(\frac{d\sigma}{dn}\right)^2 \qquad (5)$$

where the coefficient $A(T)$ is proportional to the temperature (T) according to McWhorter model[32] but independent of n. Dutta-Horn kinetics of thermal activation[33] can, however, lead to a stronger T dependence of $A(T)$.

Carrier Density (n) Dependence of Configuration Noise. The configuration noise, $\delta\sigma_c$, arises from fluctuations in the scattering cross section (Λ_c) of charge carriers. Within a "local interference" model,[26] relevant to the temperature range

in which our experiments were done, $\delta\Lambda_c \sim \Lambda_c$, which makes $\delta\sigma_c \sim \sigma l/\Lambda_c$. Here, l is the mean scattering length and $\Lambda_c \propto |v_q|^2$, where v_q is the external scattering potential. Thus

$$\frac{\delta\sigma_c^2}{\sigma^2} \sim l^2\Lambda_c^2 \sim l^2|v_q|^4 \quad (6)$$

For configuration noise arising from trapped charge redistribution, v_q is the screened Coulomb potential due to the trapped charges, implying $\delta\sigma_c$ would also be sensitive to graphene band structure. For linear bands (SLG), $q_{TF} \sim k_F \sim \sqrt{n}$, which makes, $v_q \sim 1/q_{TF} \sim 1/\sqrt{n}$. For parabolic bands (BLG/MLG), $q_{TF} \sim n^0$, making v_q independent of density. At large $|n|$, we can hence approximate the configuration noise $N_{con} \sim |n|^\gamma$, where $\gamma = -2(1 - \varepsilon)$ for SLG and 2ε for BLG. Here, ε represents the n dependence of l ($\sim|n|^\varepsilon$). For screened Coulomb,[29,30] as well as interface polar scattering,[31] $\varepsilon \sim 0-0.5$ and depends on T, as well. Below certain characteristic density n_* the charge distribution in graphene disintegrates into small puddles,[23] and the configuration noise varies weakly near the Dirac point.[24]

Since the charge exchange and configuration noise occur independently, the total normalized noise magnitude can be written as

$$S_\sigma(f)/\sigma^2 = N_{ch} + N_{con} = A(T)(d\sigma/dn)^2 + B(T)N_c(n) \quad (7)$$

where $N_c(n) = (|n|/|n_*|)^\gamma$ and 1 for $|n| < |n_*|$ and $|n| > |n_*|$, respectively. The parameters A, B, n_*, and γ were kept as fitting parameters, while $d\sigma/dn$ was obtained from the $\sigma-n$ data. Most devices exhibited significant particle-hole asymmetry, hence the electron- and hole-doped regimes were fitted separately.

Acknowledgment. We acknowledge the Department of Science and Technology (DST) for a funded project, S.R. acknowledges support under Grant No. SR/S2/CMP-02/2007. A.N.P., S.G. and V.K. thank CSIR for financial support.

REFERENCES AND NOTES

1. Novoselov, K. S.; Geim, A. K.; Morozov, S. V.; Jiang, D.; Katsnelson, M. I.; Grigorieva, I. V.; Dubonos, S. V.; Firsov, A. A. Two-Dimensional Gas of Massless Dirac Fermions in Graphene. *Nature* **2005,** *438*, 197–200.
2. Zhang, Y.; Tan, J. W.; Stormer, H. L.; Kim, P. Experimental Observation of the Quantum Hall Effect and Berry's Phase in Graphene. *Nature* **2005,** *438*, 201–204.
3. Oostinga, J. B.; Heersche, H. B.; Liu, X.; Morpurgo, A. F; Vandersypen, L. M. K. Gate-Induced Insulating State in Bilayer Graphene Devices. *Nat. Mater.* **2008,** *7*, 151–157.
4. Craciun, M. F.; Russo, S.; Yamamoto, M.; Oostinga, J. B.; Morpurgo, A. F.; Tarucha, S. Trilayer Graphene Is a Semimetal with a Gate-Tunable Band Overlap. *Nat. Nanotechnol.* **2009,** *4*, 383–388.
5. Li, X.; Wang, X.; Zhang, L.; Lee, S.; Dai, H. Chemically Derived, Ultrasmooth Graphene Nanoribbon Semiconductors. *Science* **2008,** *319*, 1229–1232.
6. Cai, J.; Ruffieux, P.; Jaafar, R.; Bieri, M.; Braun, T.; Blankenburg, S.; Muoth, M.; Seitsonen, A. P.; Saleh, M.; Feng, X.; *et al.* Atomically Precise Bottom-Up Fabrication of Graphene Nanoribbons. *Nature* **2010,** *466*, 470–473.
7. Das, A.; Pisana, S.; Chakraborty, B.; Piscanec, S.; Saha, S. K.; Waghmare, U. V.; Novoselov, K. S.; Krishnamurthy, H. R.; Geim, A. K.; Ferrari, A. C.; *et al.* Monitoring Dopants by Raman Scattering in an Electrochemically Top-Gated Graphene Transistor. *Nat. Nanotechnol.* **2008,** *3*, 210–215.
8. Xu, M.; Fujita, D.; Gao, J.; Hanagata, N. Auger Electron Spectroscopy: A Rational Method for Determining Thickness of Graphene Films. *ACS Nano* **2010,** *4*, 2937–2945.
9. Hiura, H.; Miyazaki, H.; Tsukagoshi, K. Determination of the Number of Graphene Layers: Discrete Distribution of the Secondary Electron Intensity Stemming from Individual Graphene Layers. *Appl. Phys. Exp.* **2010,** *3*, 095101–095103.
10. Jayaraman, R.; Sodini, C. G. A 1/*f* Noise Technique To Extract the Oxide Trap Density near Conduction Band Edge of Silicon. *IEEE Trans. Electron Devices* **1989,** *36*, 1773–1782.
11. Lin, Y. M.; Appenzeller, J.; Knoch, J.; Chen, Z. H.; Avouris, P. Low-Frequency Current Fluctuations in Individual Semiconducting Single-Wall Carbon Nanotubes. *Nano Lett.* **2006,** *6*, 930–936.
12. Männik, J.; Heller, I.; Janssens, A. M.; Lemay, S. G.; Dekker, C. Charge Noise in Liquid-Gated Single-Wall Carbon Nanotube Transistors. *Nano Lett.* **2008,** *8*, 685–688.
13. Lin, Y. -M.; Avouris, P. Strong Suppression of Electrical Noise in Bilayer Graphene Nanodevices. *Nano Lett.* **2008,** *8*, 2119–2125.
14. Pal, A. N.; Ghosh, A. Resistance Noise in Electrically Biased Bilayer Graphene. *Phys. Rev. Lett.* **2009,** *102*, 126805–126808.
15. Pal, A. N.; Ghosh, A. Ultralow Noise Field-Effect Transistor from Multilayer Graphene. *Appl. Phys. Lett.* **2009,** *95*, 082105–082107.
16. Shao, Q.; Liu, G.; Teweldebrhan, D.; Balandin, A. A.; Rumyantsev, S.; Shur, M. S.; Yan, D. Flicker Noise in Bilayer Graphene Transistors. *IEEE Electron Device Lett.* **2009,** *30*, 288–290.
17. Lui, G; Stillman, W.; Rumyantse, S.; Shao, Q.; Shur, M.; Balandin, A. A. Low-Frequency Electronic Noise in the Double-Gate Single Layer Graphene Transistors. *Appl. Phys. Lett.* **2009,** *95*, 033103.
18. Heller, I.; Chatoor, S.; Mannik, J.; Zevenbergen, M. A. G.; Oostinga, J. B.; Morpurgo, A. F.; Dekker, C.; Lemay, S. G. Charge Noise in Graphene Transistors. *Nano Lett.* **2010,** *10*, 1563–1567.
19. Xu, G.; Torres, C. M., Jr.; Zhang, Y.; Liu, F.; Song, E. B.; Wang, M.; Zhou, Y.; Zeng, C.; Wang, K. L. Effect of Spatial Charge Inhomogeneity on 1/*f* Noise Behavior in Graphene. *Nano Lett.* **2010,** *10*, 3312–3317.
20. Rumyantsev, S.; Liu, G.; Stillman, W.; Shur, M.; Balandin, A. A. Electrical and Noise Characteristics of Graphene Field-Effect Transistors: Ambient Effects and Noise Sources. *J. Phys.: Condens. Matter* **2010,** *22*, 395302.
21. Cheng, Z.; Li, Q.; Li, Z.; Zhou, Q.; Fang, Y. Suspended Graphene Sensors with Improved Signal and Reduced Noise. *Nano Lett.* **2010,** *10*, 1864–1868.
22. Tersoff, J. Low-Frequency Noise in Nanoscale Ballistic Transistors. *Nano Lett.* **2007,** *7*, 194–198.
23. Martin, J.; Akerman, N.; Ulbricht, G.; Lohmann, T.; Smet, J. H.; von Klitzing, K.; Yacoby, A. Observation of Electron–Hole Puddles in Graphene Using a Scanning Single-Electron Transistor. *Nat. Phys.* **2008,** *4*, 144–148.
24. Pal, A. N.; Bol, A. A.; Ghosh, A. Large Low-Frequency Resistance Noise in Chemical Vapor Deposited Graphene. *Appl. Phys. Lett.* **2010,** *97*, 133504–133506.
25. Ghosh, A.; Kar, S.; Bid, A.; Raychaudhuri, A. K. A Set-Up for Measurement of Low Frequency Conductance Fluctuation (Noise) Using Digital Signal Processing Techniques; e-print arXiv:condmat/0402130v1, 2004.
26. Pelz, J.; Clarke, J. Quantitative "Local-Interference" Model for 1/*f* Noise in Metal Films. *Phys. Rev. B* **1987,** *36*, 4479–4482.
27. Huard, B.; Stander, N.; Sulpizio, J. A.; Goldhaber-Gordon, D. Evidence of the Role of Contacts on the Observed Electron–Hole Asymmetry in Graphene. *Phys. Rev. B* **2008,** *78*, 121402(R).
28. Zhu, W.; Perebeinos, V.; Freitag, M.; Avouris, P. Carrier Scattering, Mobilities, and Electrostatic Potential in Monolayer, Bilayer, and Trilayer Graphene. *Phys. Rev. B* **2009,** *80*, 235402.
29. Adam, S.; Hwang, E. H.; Galitski, V. M.; Das Sarma, S. A Self-Consistant Theory for Graphene Transport. *Proc. Natl. Acad. Sci. U.S.A.* **2007,** *104*, 18392–18397.
30. Adam, S.; Das Sarma, S. Boltzmann Transport and Residual Conductivity in Bilayer Graphene. *Phys. Rev. B* **2008,** *77*, 115436.
31. Chen, J.-H.; Jang, C.; Xiao, S.; Ishigami, M.; Fuhrer, M. S. Intrinsic and Extrinsic Performance Limits of Graphene Devices on SiO_2. *Nat. Nanotechnol.* **2008,** *3*, 206–209.
32. McWhorter, A. L. *Semiconductor Surface Physics*; University of Pennsylvania Press: Philadelphia, 1957; p 207.
33. Dutta, P.; Horn, P. M. Low-Frequency Fluctuations in Solids: 1/*f* Noise. *Rev. Mod. Phys.* **1981,** *53*, 497–516.